

000000044770004438896

UC-25
LBL-5770 C-1

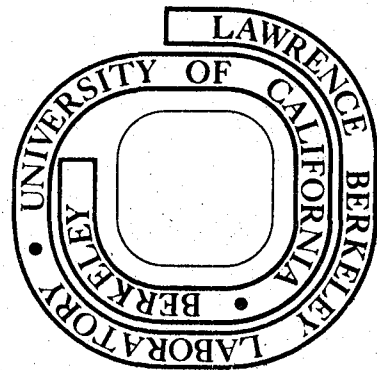
LIQUID PHASE SINTERING OF IRON WITH COPPER
BASE ALLOY POWDERS

Meng-Hsiu Chen
(M. E. thesis)

December 1976

Prepared for the U. S. Energy Research and
Development Administration under Contract W-7405-ENG-48

For Reference
Not to be taken from this room



LBL-5770 C-1

LEGAL NOTICE

This report was prepared as an account of work sponsored by the United States Government. Neither the United States nor the United States Energy Research and Development Administration, nor any of their employees, nor any of their contractors, subcontractors, or their employees, makes any warranty, express or implied, or assumes any legal liability or responsibility for the accuracy, completeness or usefulness of any information, apparatus, product or process disclosed, or represents that its use would not infringe privately owned rights.

LIQUID PHASE SINTERING OF IRON WITH COPPER
BASE ALLOY POWDERSCONTENTS

	<u>Page</u>
ABSTRACT.....	i
I. Introduction.....	1-3
II. Materials and Experimental Methods	
A. Powder Characteristics.....	4
B. Blending and Compaction.....	5
C. Sintering Environment.....	5
D. Temperature Measurement.....	6
E. Volume and Density Measurement.....	6
F. Metallography.....	6
G. Mechanical Property Tests.....	7
III. Results and Discussion	
A. Densification.....	9
B. Tensile and Transverse Rupture Strength.....	10
C. Microhardness.....	11
D. Microscopic Examination.....	12-13
IV. Conclusions.....	14
ACKNOWLEDGEMENTS.....	15
REFERENCES.....	16-17
FIGURE CAPTIONS.....	18-19
FIGURES.....	20-38



000000044770004139818

LIQUID PHASE SINTERING OF IRON WITH COPPER BASE ALLOY POWDERS

By

Meng-Hsiu Chen

Materials and Molecular Research Division
Lawrence Berkeley Laboratory
and Department of Mechanical Engineering
University of California
Berkeley, California 94720

ABSTRACT

The physical and mechanical properties of a series of atomized elemental Fe and prealloyed Fe + Cu powders blended with different amounts of liquid phase additions were studied in the as-sintered condition.

The alloy of 88% Cu, 3% Mn, 9% Si was found to have superior characteristics for use as a liquid phase material in the sintering of elemental Fe or its prealloyed powders. The effects of additions of this alloy on the sintered density, tensile strength, transverse rupture strength and hardness were determined and compared with other reported results.

The sintering mechanism and swelling effect did not conform with conventional theories. Some recommendations are made for further studies in liquid phase sintering of ferrous systems.

I. INTRODUCTION

The primary objective of this study was to develop a low melting master alloy material to be used as a liquid phase in the sintering of Fe compacts. In the simple process of pressing and sintering, a compact without the presence of some liquid phase can only reach a sintered density of about 90% of theoretical. It has been found that the residual porosity has many deleterious effects on the mechanical properties of parts made by powder metallurgy techniques. Other processes to produce high density parts such as high compacting pressure, forging, hot isostatic pressing, sinter-repress-resinter and infiltration are all comparatively higher in cost or involve more elaborate procedures. Therefore, a need exists for an improvement in the simple press-sinter techniques to achieve better density and strength. Liquid phase sintering could be a simple way to satisfy this need.

Copper and copper base alloys have been widely used in the industry either as a base material or as an infiltrant for ferrous components. Mixtures of iron and copper powders are commonly used to produce high strength steel parts. Copper powders, at supersolidus sintering temperatures, melt and wet the iron particles and bind them tightly together after solidification. The sintering behavior of Fe + Cu alloys made from mixed elemental powders has been well documented by many authors since 1946.¹⁻⁶ A disadvantage of

copper additions is "copper growth" (swelling) during sintering which reduces the sintered density and dimensional accuracy. The cause and the effect of this phenomenon have also been extensively studied. G. Bockstiegel^{7,8} and T. Krantz⁹ have given a good review on this subject. However, a controversy still remains in the interpretation of the cause of the "copper growth" in Fe + Cu mixtures. Investigators believe swelling is caused by (i) volume diffusion of copper into iron particles, (ii) penetration of liquid copper between the iron particles, or (iii) penetration of molten copper into the grain boundaries of the iron particles. Recently, Berner, Exner and Petzow,¹⁰ Trudel and Angers,¹¹ concluded that the "copper growth" is too rapid to be caused by volume diffusion and proved that the rapid expansion observed at the melting point of Cu is caused by the penetration of copper in the boundaries within and between Fe particles. Pure copper has a melting temperature of 1083°C; therefore, a higher temperature is required for the molten copper to wet and flow freely through the interconnected pores in the pressed compacts. After studying the copper base binary and ternary phase diagrams, it was found that some alloys have much lower melting temperatures, e.g., 870°C for Cu-Mn and 858°C for Cu-Si. The temperature of the peritectic reaction, $\alpha + \text{melt} \rightleftharpoons \beta$ (852°C, ~ 5.25% Si), decreases suddenly to 760°C upon the addition of 2.5% Mn.¹² In a search for a material that would alloy

rapidly during short sintering cycles and would be compatible with existing equipment and practices, it was found from this study that the system of Cu-Mn-Si offered many advantages such as a low melting point, fast diffusion rate, and greater hardenability. In the present study, an alloy composed of 88% Cu, 3% Mn and 9% Si was chosen as an additive to provide a liquid phase during sintering. For brevity, this composition will be referred to as Cu-Mn-Si. It is an intermetallic compound that melts at 780°C.

II. MATERIALS AND EXPERIMENTAL METHODS

A. Powder Characteristics:

Characteristics of the elemental and prealloyed powders used in this study are shown as manufacturer's data in the following table.

	Elemental Fe*	Prealloyed Fe**
Chemical Analysis - Cu	0	11.86
(wt. %) - C	0.01	0.02
- S	0.01	0.012
- P	0.005	0.01
- Mn	0.2	0
- Si	0.02	0
- Fe	Balance	Balance
H ₂ loss	0.12	0.67
Screen analysis	%	%
-80+100	2.0	6.3
-100+150	14.0	19.2
-150+200	22.0	23.8
-200+250	10.0	11.4
-250+325	22.0	11.1
-325	30.0	28.2
Apparent Density	2.95 g/cm ³	2.91 g/cm ³
Flow time	25 sec/50g	24.5 sec/50g

* EMP atomized, grade 300M, A. O. Smith Company

** Preinfiltrated. Prefiltron 12, Pfizer Company

The above two powders were chosen because of their similarity in particle size distribution and physical properties. The Cu-Mn-Si alloy was cast into an ingot which was crushed and then ball milled to $1 \sim 8 \mu$ size. X-ray examination showed the alloy to be an intermetallic compound with a structure similar to Cu_3Si . The compound had a silvery luster and was very brittle in spite of the large Cu content. The measured density was 7.85g/cm^3 .

B. Blending and Compacting

Carefully weighed powders, together with alumina pellets, were contained in glass jars and tumble blended for sixty minutes. The alumina pellets sufficiently broke up agglomerated powders and aided in producing a uniform powder mixture. Figure 1 shows a pressed compact with fine Cu-Mn-Si powders well distributed around coarse Fe particles. After blending, each mixture of powders was pressed in a double acting steel die, using a hydraulic press. Every compact was held under pressure over two minutes to allow for outgassing. All die surfaces were lubricated before each compacting process. The lubricant used was a mixture of 100g of zinc stearate in one liter of methylchloroform (1.1.1-trichloroethane).

C. Sintering Environment

All samples after compacting were sintered in a hydrogen furnace (Fig. 2). A Matheson 8362 Purifier operating at 725°F was used to purify the H_2 before it went into the furnace. Purified H_2 provides a good reducing atmosphere for sintering and excludes the carburization effect by the

CO content in other available sintering atmospheres.¹³ To assure that the fresh flowing H₂ was in contact with the sample surfaces, the compact was put in a cylindrical crucible with meshed ends and the furnace was pressurized to 6 ~ 8 psi over atmospheric pressure. Some sinterings were performed in a closed bottom crucible which resulted in a noncirculating atmosphere at the bottom of the crucible and thus left some visible oxides on the sample surfaces after sintering. This suggests that the positioning of compacts during sintering must be carefully designed to allow a good fresh flowing atmosphere all over the sample surfaces.

D. Temperature Measurement

A Chromel-Alumel "Type K" thermocouple sealed in a protection tube was used to measure the sintering temperature. This thermocouple was set at the middle of the furnace hot zone together with the sample during the entire sintering period.

A digital indicator (Type K/°C) was used to read the temperature and an x-y recorder was used to calculate the heating and cooling rate, and to determine the melting point of the liquid phase.

E. Volume and Density Measurement

A volume displacement method was used to measure the volume and density of the green or sintered compacts. Before immersing the compacts in the water they were first

microscope, the nonconductive epoxy in the pores would be charged by the electron beam and cause the fluorescent emission to degrade the contrast of the picture. Samples were also prepared for hot stage scanning electron microscopy to directly observe the formation and flow of the liquid phase during sintering. Electron microprobe analysis was used to investigate the distribution of each alloying element in the sintered compact.

G. Mechanical Property Test

Sintered tensile test bars conforming to MPIF standard 10-63, Fig. 3, were tested with an Instron testing machine using a crosshead speed of 0.05 cm/min. ASTM standard E8 was used to choose gripping devices and methods of determining tensile strength and elongation. Transverse rupture test bars conforming to MPIF standard 13-62, Fig. 4, were also tested with the Instron testing machine using a three point bending fixture, Fig. 5. A Leitz Wetzlar miniload hardness tester was used to determine the hardness of the sintered parts.

III. RESULTS AND DISCUSSIONS

A. Densification

The effect of Cu-Mn-Si content on the green density of Fe compacts is shown in Fig. 6. The decrease in the green density at higher Cu-Mn-Si additions in the EMP elemental Fe powder compacts was due to the incompressibility of the Cu-Mn-Si. This can be explained by the high hardness (630VH) of the intermetallic compound. Because of the varying green density, the densification results could be compared either to the compacting pressure or to the green density. Shown in Figs. 7, 8 and 9, are the effects of different Cu-Mn-Si additions on the sintered densities under different compacting pressures. Figures 10, 11 and 12, show green density vs. sintered density with different Cu-Mn-Si additions. Combining the above results, it was found that densification happened most effectively at a sintering temperature of about 1150°C. Figure 13 shows the temperature effects on sintered densities. In this figure, the samples were compared based on identical green densities of 6.0 g/cm³ without considering their compacting pressure. The increasing density at increasing liquid phase addition resembles the Fe + Cu system reported by many authors, but with a higher degree of densification at the same amount of addition and the same sintering condition. A swelling of the compacts occurred when sintering with 10% Cu-Mn-Si or less. This is very similar to the "copper growth" in the elemental Fe - Cu system. The

densification results of sintering prealloyed Fe - Cu powder compacts with various amount of Cu-Mn-Si additions are shown in Fig. 14. In this prealloyed system, the "swelling" phenomenon did not appear because the powders were already saturated with copper. The copper prevented the penetration of molten liquid into the grain boundaries and limited further diffusion of copper into iron particles, thus eliminating the cause of "swelling". A good densification result of 99% of the theoretical density was achieved by sintering: 1) EMP Fe and 30% Cu-Mn-Si at 1050°C for four hours in a H₂ atmosphere; 2) EMP Fe and 40% Cu-Mn-Si at 1150°C for one hour; 3) EMP Fe and 30% Cu-Mn-Si at 1350°C for five minutes, or 4) prealloyed powder and 10% Cu-Mn-Si at 1150°C one hour.

B. Tensile Strength and Transverse Rupture Strength

The tensile test specimens were compacted at a relatively low pressure of 60 ksi. Knowing from the above discussions that higher densities and thus better properties were achieved by increasing the compacting pressure or green density, the tensile strength can be expected to be higher than the data presented here. From Fig. 15, it can be seen that the tensile strength of EMP Fe compacts increased with increasing Cu-Mn-Si content up to a limit of about 20% and then leveled off. Further increases in liquid phase content increased the sintered density but not the tensile strength. The tensile strength of the prealloyed powder compacts was increased extensively by the addition of Cu-Mn-Si and reached a maximum at about 10%

wt. content. More Cu-Mn-Si increased the sintered density but decreased the ultimate tensile strength. This may appear to be contradictory to the conventional assumption of increasing mechanical properties with increasing density. However, care must be taken when making a comparison. The assumption held true when comparing samples of the same material compositions. A shift in composition may have had a weakening effect large enough to overcome the strengthening effect of higher density. This is shown by the drop of ultimate tensile strength and transverse rupture strength in a prealloyed powder compact with more than 10% Cu-Mn-Si content. Transverse rupture test specimens were sintered at the same conditions as the tensile specimens, but a higher compacting pressure of 80 ksi was used. The results are shown in Fig. 16. The transverse rupture strength of EMP compacts also increased with increasing Cu-Mn-Si content up to about 20% and then leveled off as in the case of tensile strength. The prealloyed powder compacts also showed a maximum of T.R.S. at about 10% Cu-Mn-Si addition and then started to decrease with larger additions. A careful analysis showed that all the mechanical properties reached a maximum at about 20% total copper content.

C. Microhardness

By using a Leitz miniload hardness tester with a 50 gram load the hardness of EMP iron particles in the green compact was found to be 120 VH. The pure EMP compacts after

sintering had an annealed hardness of 64 VH which is considered typical for a very soft and ductile material. Cu-Mn-Si had a much higher hardness of 678 VH as may be expected for an intermetallic compound. The soft EMP powder was mixed with some hard Cu-Mn-Si powder and sintered at a temperature high enough to melt the Cu-Mn-Si. During sintering, diffusion and solution-precipitation took place. Iron particles were solution strengthened by dissolving most of the silicon and a limited amount of copper and manganese. This resulted in strong particles with a hardness of 465 VH. The originally hard Cu-Mn-Si was softened by losing most of its silicon content and some of its copper and manganese to iron. The result was a soft matrix of 106 VH. The final sintered compact consisted of hardened Fe particles bonded by a soft copper base matrix. This is a desirable structure for parts as-sintered and a good base structure for further forging¹⁵ or additional processing. The detail composition and hardness in each phase after sintering is shown in Fig. 17.

D. Microscopic Examination

A hot stage electron microscope was used to study the liquid phase behavior during sintering by direct observation. A green compact of Fe - 30% Cu-Mn-Si was subjected to a heating rate of 12°C/min under vacuum in the hot stage. Before reaching 780°C, only thermal expansion was noticed because all the particles kept their relative positions, but with increased distances between each other. Above 780°C, Cu-Mn-Si particles

started to melt and the liquid phase fraction increased with temperature. During this stage, the pore size, shape, and distribution started to change. The drastic rearrangement and shrinkage happened only upon complete melting of the Cu-Mn-Si particles at 1020°C. At this temperature, the Fe particles no longer kept their relative positions and all the pores closed in less than 10 seconds. Small shiny flakes of oxides could be observed floating on the liquid surface.

The reaction between Fe particles and the alloying elements was studied by using electron microprobe analysis. Figures 18 and 19 show the microstructure of two samples sintered for five minutes and four hours respectively at 1150°C in a H₂ atmosphere. Both samples have three different phases present. From the EDAX X-ray profile analysis (Fig. 17), it was found that during sintering the diffusion process and boundary penetration were nearly completed within five minutes. The longer sintering time contributed to particles rearranging, and pores closing, spheroidizing and coalescing. The fact that diffusion and boundary penetration happen before rearrangement indicates the reverse of the conventional theory of liquid phase sintering,¹⁶ which assumed that the rearrangement is the first stage before the solution-precipitation or diffusion process.

IV. CONCLUSION

1. High sintered density of 7.82 g/cm^3 (over 99% of the theoretical value) can be achieved in the sintering of EMP iron compacts by adding Cu-Mn-Si as a liquid phase. If pre-alloyed Fe - Cu is employed as a base, similar densification can be achieved by adding only 10% Cu-Mn-Si and sintering at 1150°C for one hour in H_2 atmosphere.
2. The fast diffusion of silicon and some limited amount of copper and manganese into iron particles contributes to better mechanical properties through solution strengthening. The ultimate tensile strength and transverse rupture strength increase markedly with the addition of Cu-Mn-Si to both elemental and prealloyed iron compacts. Maximum strengths occur at about 20% total copper content. The compacts made from pre-alloyed powder have substantially greater tensile and transverse rupture strengths. A tensile strength of 102 ksi and a transverse rupture strength of 188 ksi can be obtained from the prealloyed compacts.
3. Swelling of compacts is observed during sintering of EMP elemental iron compacts with Cu-Mn-Si additions up to 10%. This is very similar to the "copper growth" observed with elemental iron and copper mixtures. The only difference is that Cu-Mn-Si diffuses very rapidly. Therefore, both diffusion and boundary penetration contribute to the "swelling" of the compacts.
4. The resulting structure of hardened iron particles bonded by a soft copper base matrix is very desirable for as-sintered parts.

5. Manganese and silicon are beneficial alloying elements in steel design. Their contributions in regard to heat-treatability can be expected to improve the mechanical properties reported in this study.

An investigation of optimal addition of Cu-Mn-Si and heat-treatability is recommended for further studies in this area.

Acknowledgement

The author is sincerely grateful to Prof. Milton R. Pickus for his advice and guidance throughout the project. Special thanks to Dr. John Ling-Fai Wang for his patient encouragement and valuable direction which contributed substantially to this report. The technical assistance rendered by Mr. John T. Holthuis and Mr. John A. Jacobsen and the many people within the Materials and Molecular Research Division is greatly appreciated.

This work was performed under the auspices of the U.S. Energy Research and Development Administration through the Materials and Molecular Research Division, University of California, Berkeley California.

REFERENCES

1. V. N. Eremenko and Y. V. Naidich, "Liquid-Phase Sintering", (a special research report) (1970).
2. F. C. Kelley, Iron Age, 158, 57 (1946).
3. L. Northcott and C. J. Leadbeater, "Sintered Iron Copper Compacts", Symposium on Powder Metallurgy - The Iron and Steel Inst. Spec. Report, 38, 142 (1947).
4. J. F. Kuzmick and E. N. Mazza, "Studies on Control of Growth of Shrinkage of Iron - Copper Compacts During Sintering", J. of Metals, 188, 1218 (1950).
5. P. U. Gummeson and L. Fross, "How Dimensions and Properties are Affected by Adding Copper to Iron Powder Compacts", Proc. 11th Ann. Meeting Metal Powder Assoc., 56, (1955).
6. J. E. Elliot, "Metallurgia", 59, 17 (1959).
7. G. Bockstiegel, "Nature and Cause of Volume Changes in the Sintering of Fe-Cu and Fe-Cu-C Powder Compacts", Stahl und Eisen, 79, 1187 (1959).
8. G. Bockstiegel, "Metallurgia", III (4), 67 (1962).
9. T. Krantz, "Effect of Density and Composition on the Dimensional Stability and Strength of Fe-Cu Alloys", Int. J. of P/M, 5 (3), (1969).
10. D. Berner, H. E. Exner and G. Petzow, "Swelling of Fe-Cu Mixtures During Sintering and Infiltration", Modern Development in P/M, 6, 273 (1973).
11. Y. Trudel and R. Angers, "Properties of Fe-Cu Alloys Made from Elemental or Prealloyed Powders", 11 (1), 5 (1975).

12. C. S. Smith and W. R. Hibbard, Trans. Amer. Inst. Min. Met. Eng., 147, 222 (1942).
13. L. A. Zagorski and E. J. Eckel, "The Effect of the Furnace Atmosphere on the Infiltration of Fe-Cu Compacts", Int. K. of P/M, 7 (2), 41 (1971).
14. J. Klein, (M.S. Thesis), "A Preliminary Investigation of Liquid Phase Sintering in Ferrous Systems", MMRD-LBL, Dept. of Mech. Eng., U.C. Berkeley, (1975).
15. H. E. Fischmeister and L-E. Larsson, "Fast Diffusion Alloying for Powder Forging Using a Liquid Phase", Powder Metallurgy, 17 (33), 227 (1974).
16. H. S. Cannon and F. V. Lenel, "Some Observations on Mechanism of Liquid Phase Sintering", Plansee Seminar 1952, F. Benesovsky (Ed.), Metallwerk Plansee, Reutte, 106 (1953).

FIGURE CAPTIONS

- Fig. 1. Green compact of course Fe particles mixed with 30% fine Cu-Mn-Si powders.
- Fig. 2. Schematic diagram of hydrogen furnace.
- Fig. 3. MPIF Standard 10-63 tensile test specimen.
- Fig. 4. Die and punches for making MPIF Standard 13-62 transverse rupture test specimens.
- Fig. 5. Fixture for transverse rupture test.
- Fig. 6. The effect of Cu-Mn-Si additions to elemental iron on green density at different compacting pressures.
- Fig. 7. The effect of Cu-Mn-Si content on sintered density. (1050°C) - Elemental iron.
- Fig. 8. The effect of Cu-Mn-Si content on sintered density. (1150°C) - Elemental iron.
- Fig. 9. The effect of Cu-Mn-Si content on sintered density. (1250°C) - Elemental iron.
- Fig. 10. Sintered density vs. green density for compacts sintered at 1050°C. Elemental iron.
- Fig. 11. Sintered density vs. green density for compacts sintered at 1150°C. Elemental iron.
- Fig. 12. Sintered density vs. green density for compacts sintered at 1250°C. Elemental iron.
- Fig. 13. Effect of sintering temperature on sintered density.
- Fig. 14. Sintered density of elemental and prealloyed Fe powders.
- Fig. 15. Ultimate tensile strength of elemental and prealloyed Fe powder compacts.

Fig. 16. Transverse rupture strength of elemental and pre-alloyed Fe powder compacts.

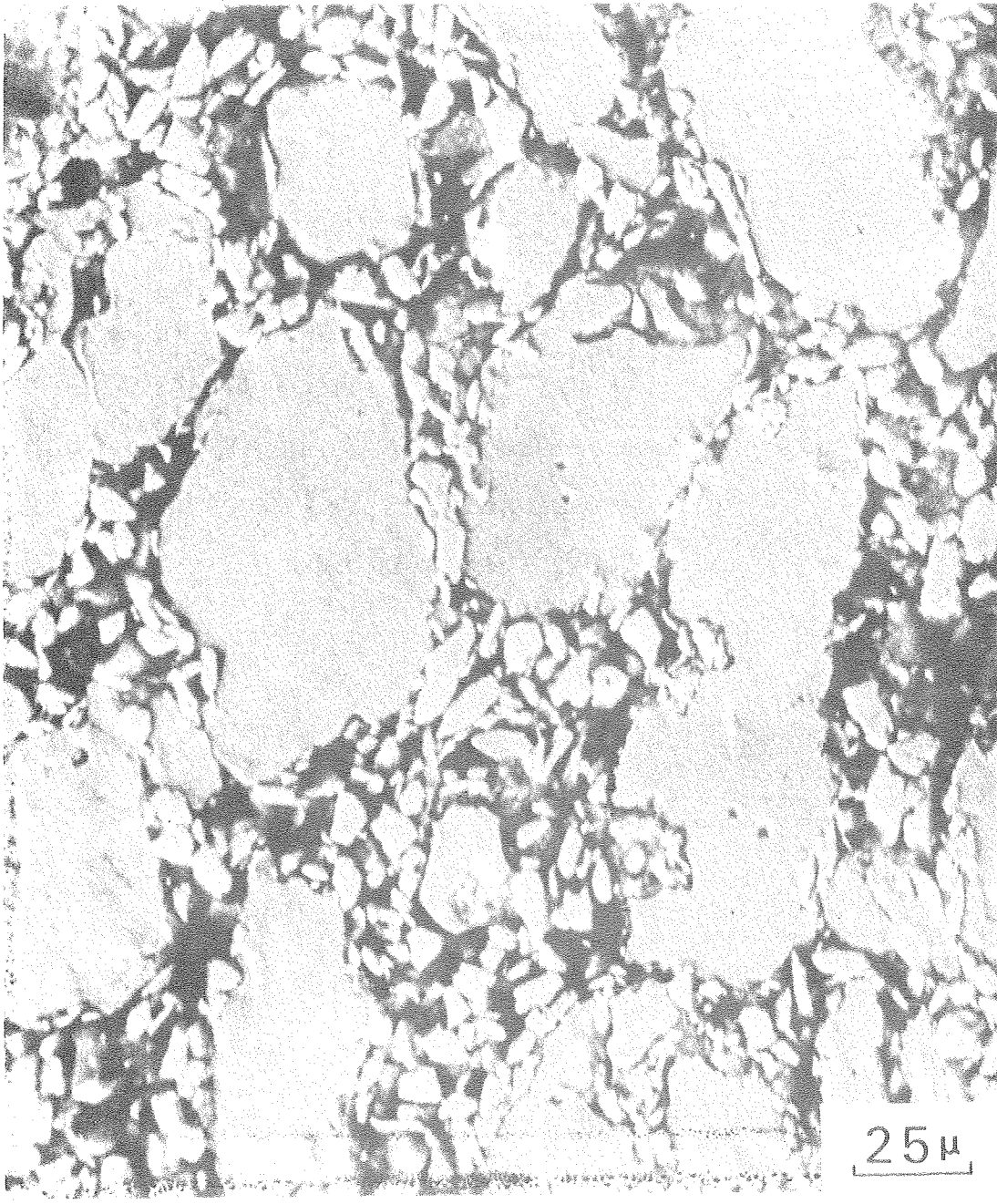
Fig. 17. EMP elemental Fe powder mixed with 30% Cu-Mn-Si and sintered at 1050°C for 5 minutes and 4 hours.

EDAX X-ray profile analysis of the three phases present.

Fig. 18. Microstructure of EMP elemental Fe powder mixed with 30% Cu-Mn-Si and sintered at 1050°C for 5 minutes.

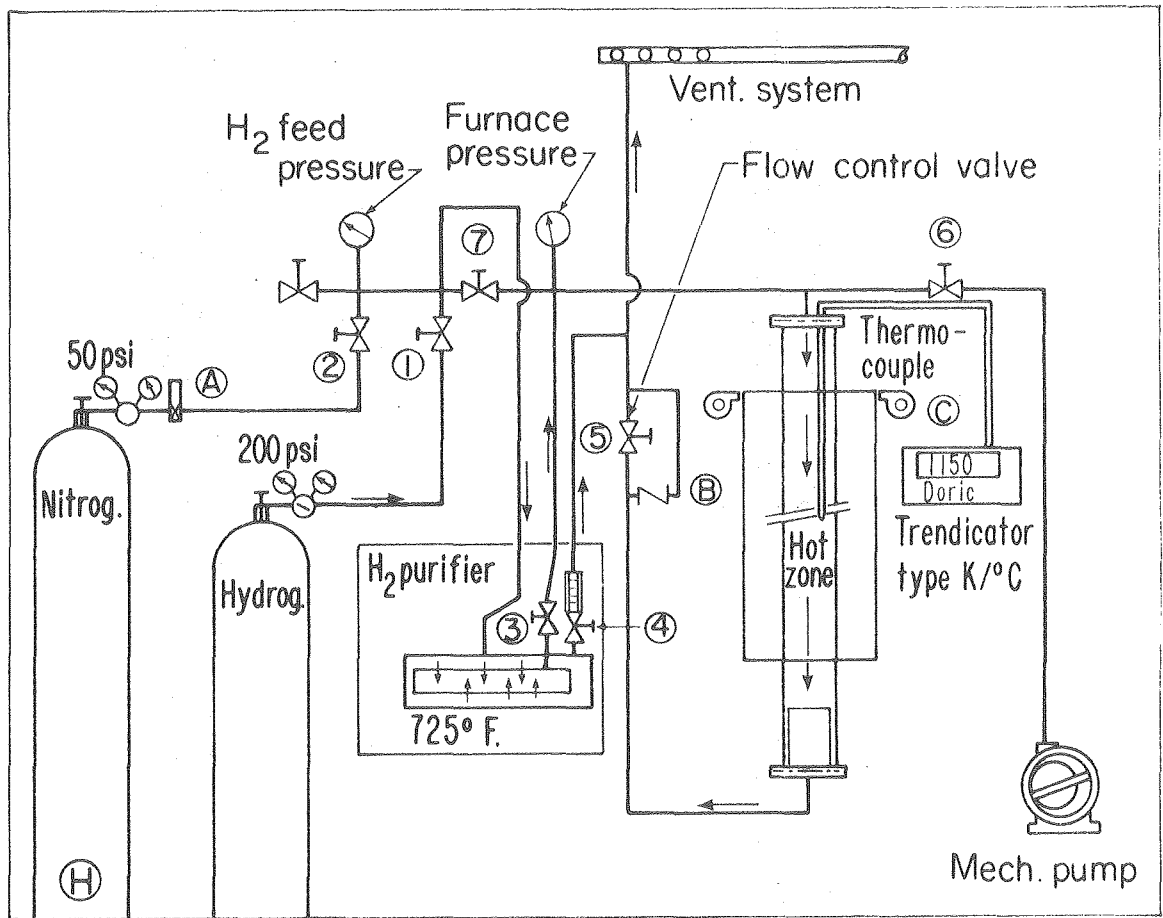
Fig. 19. Microstructure of EMP elemental Fe powder mixed with 30% Cu-Mn-Si and sintered at 1050°C for 4 hours.

(a). 600X, (b). 150X.



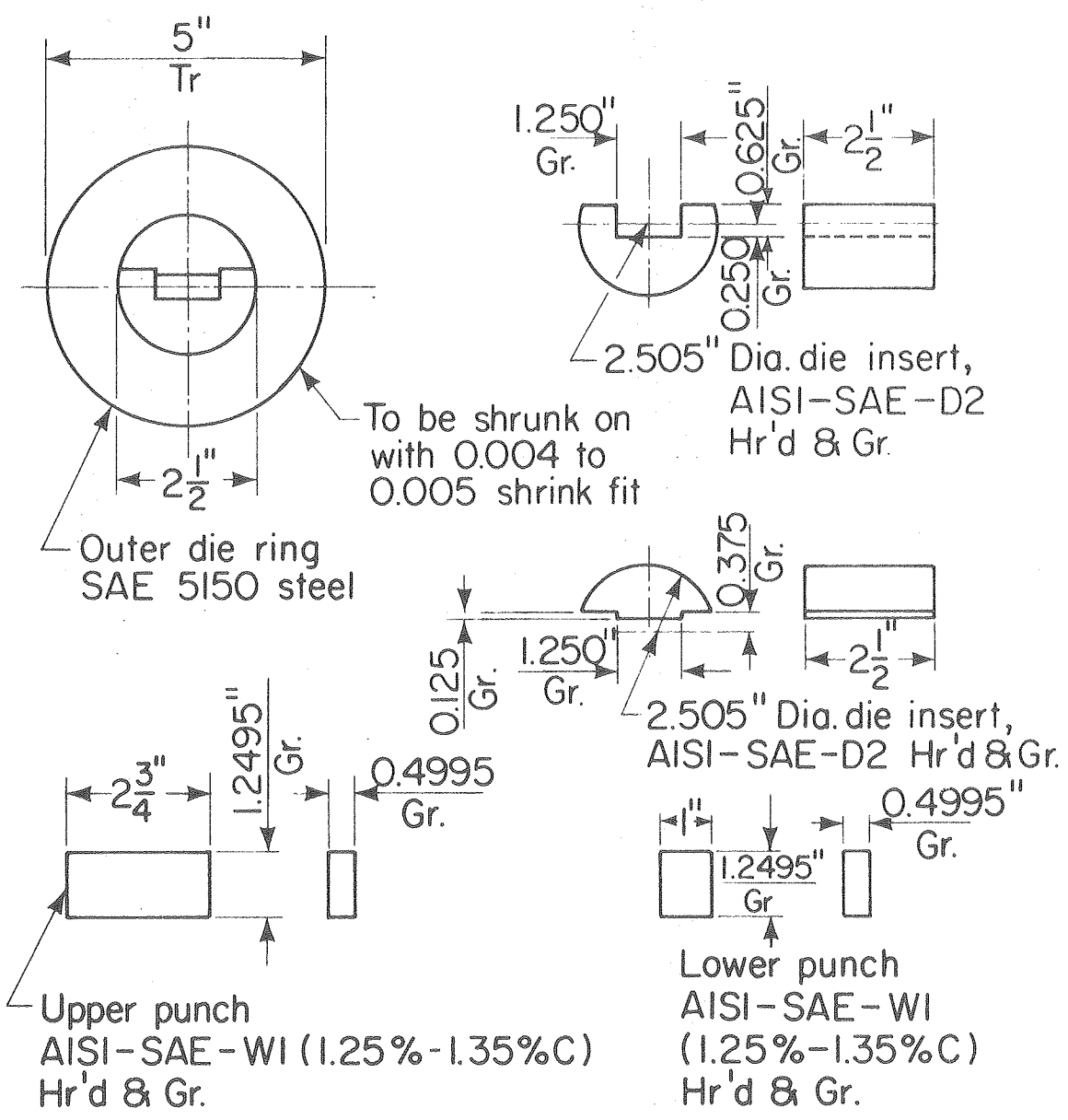
XBB 760-11751

Fig. 1



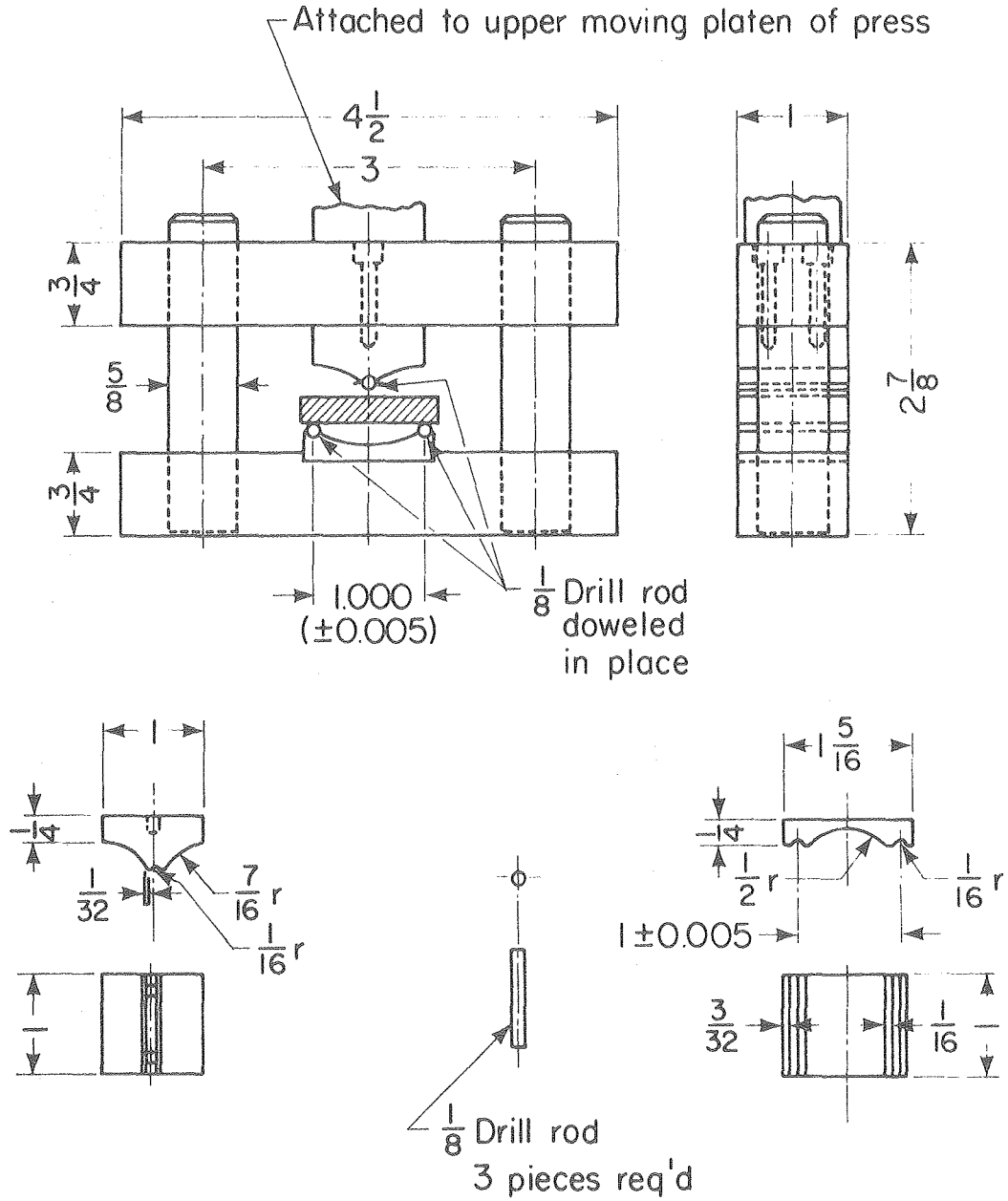
XBL 772 - 355

Fig. 2



XBL 772-358

Fig. 4

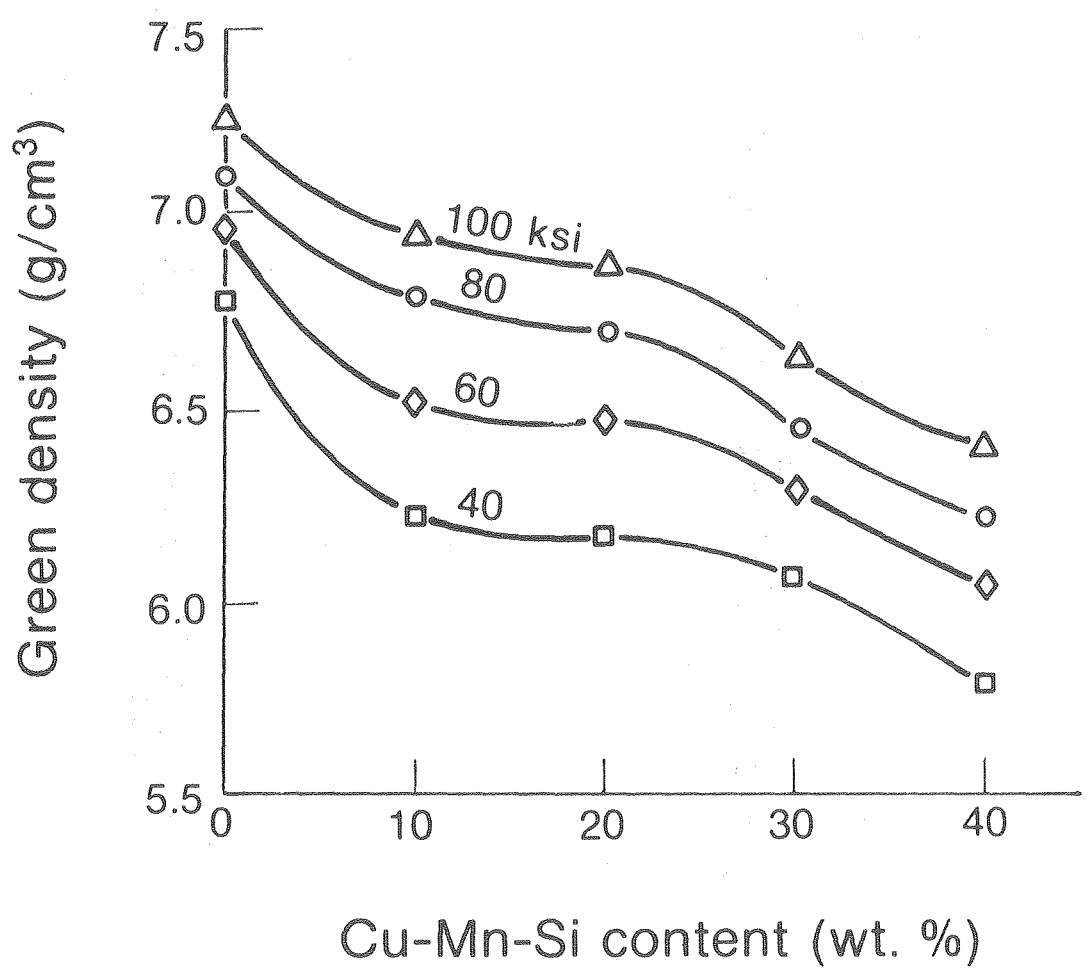


Details of fixture for testing bending strength

All dimensions in inches.

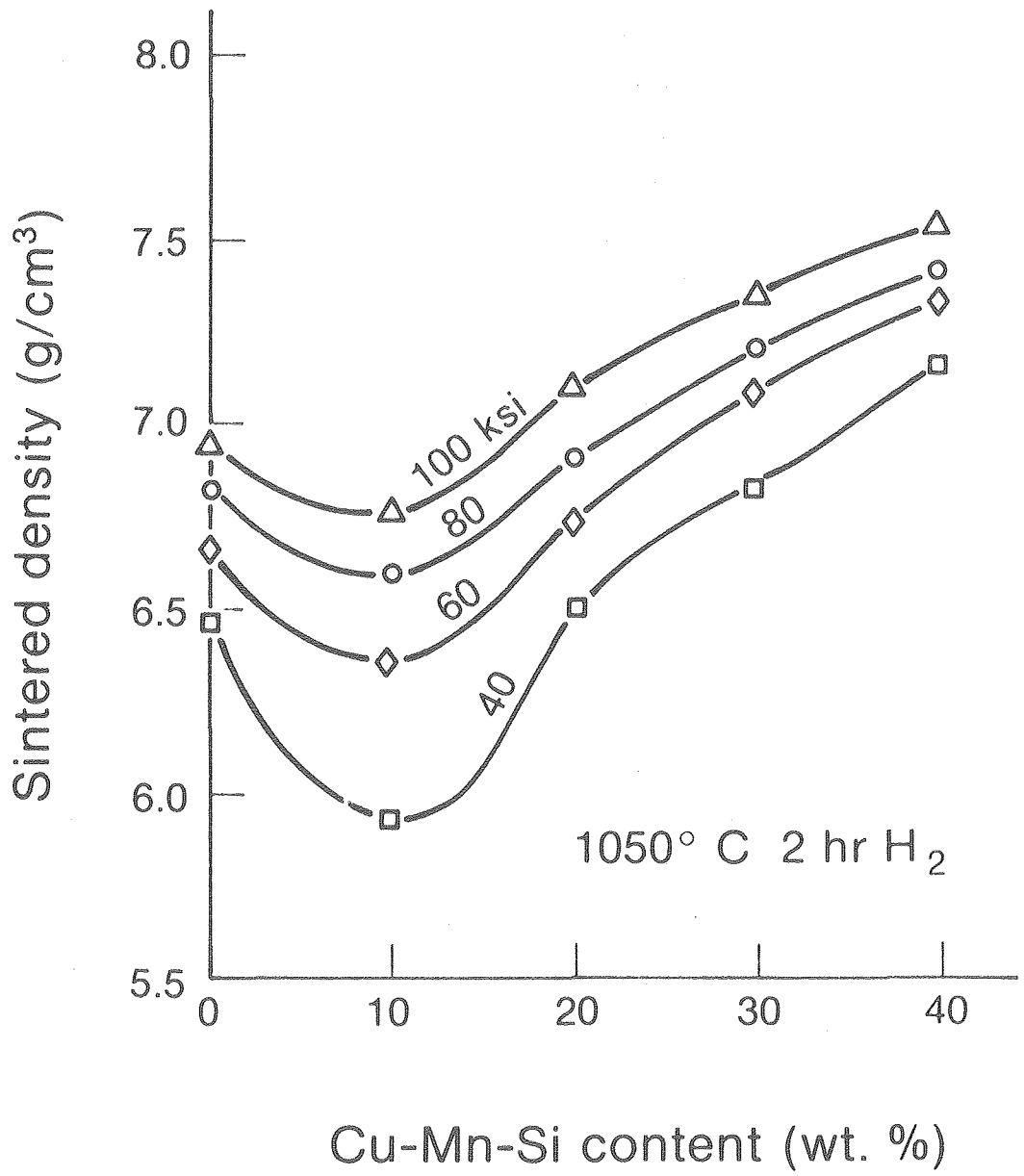
XBL 772-357

Fig. 5



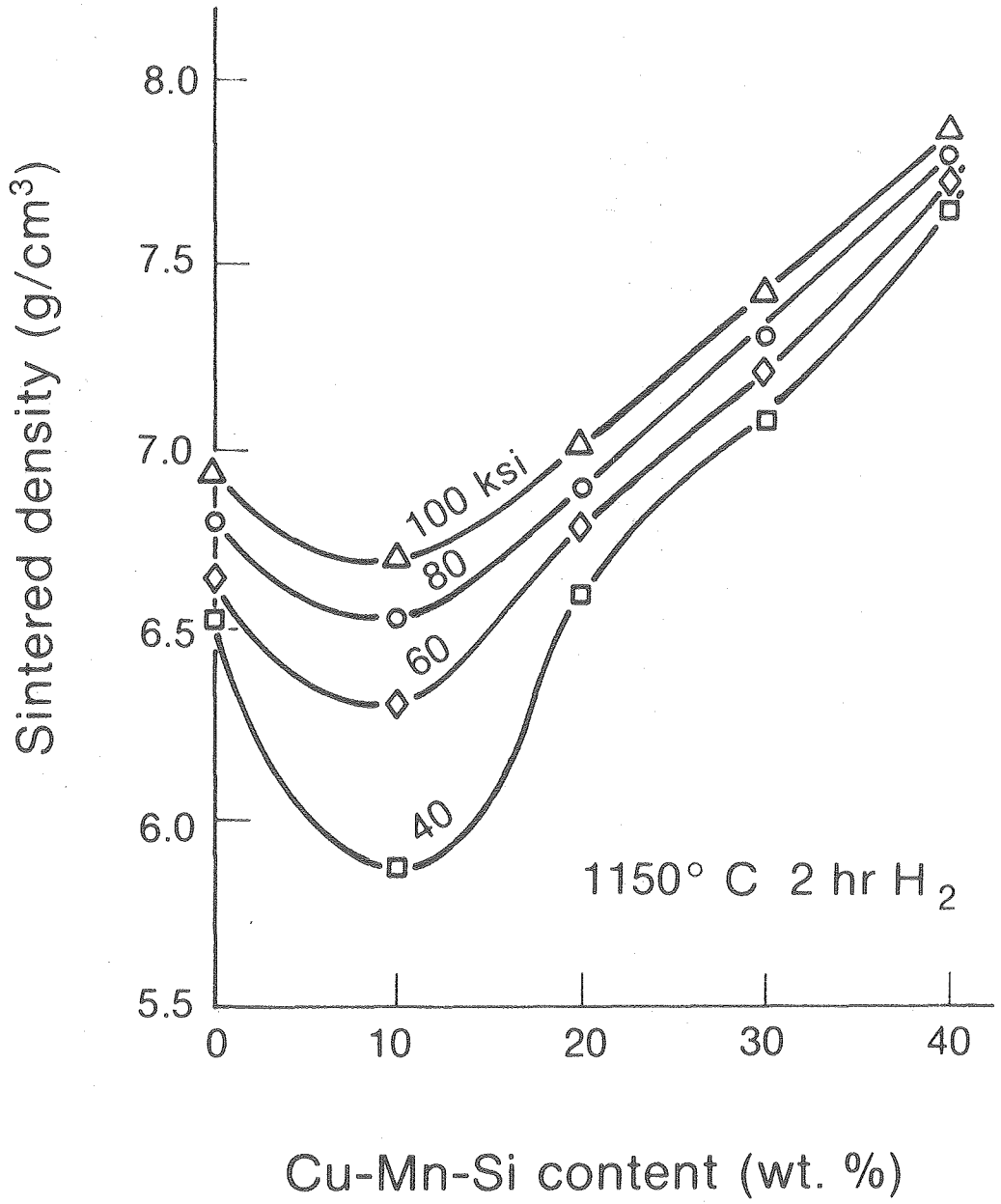
XBL 772-352

Fig. 6



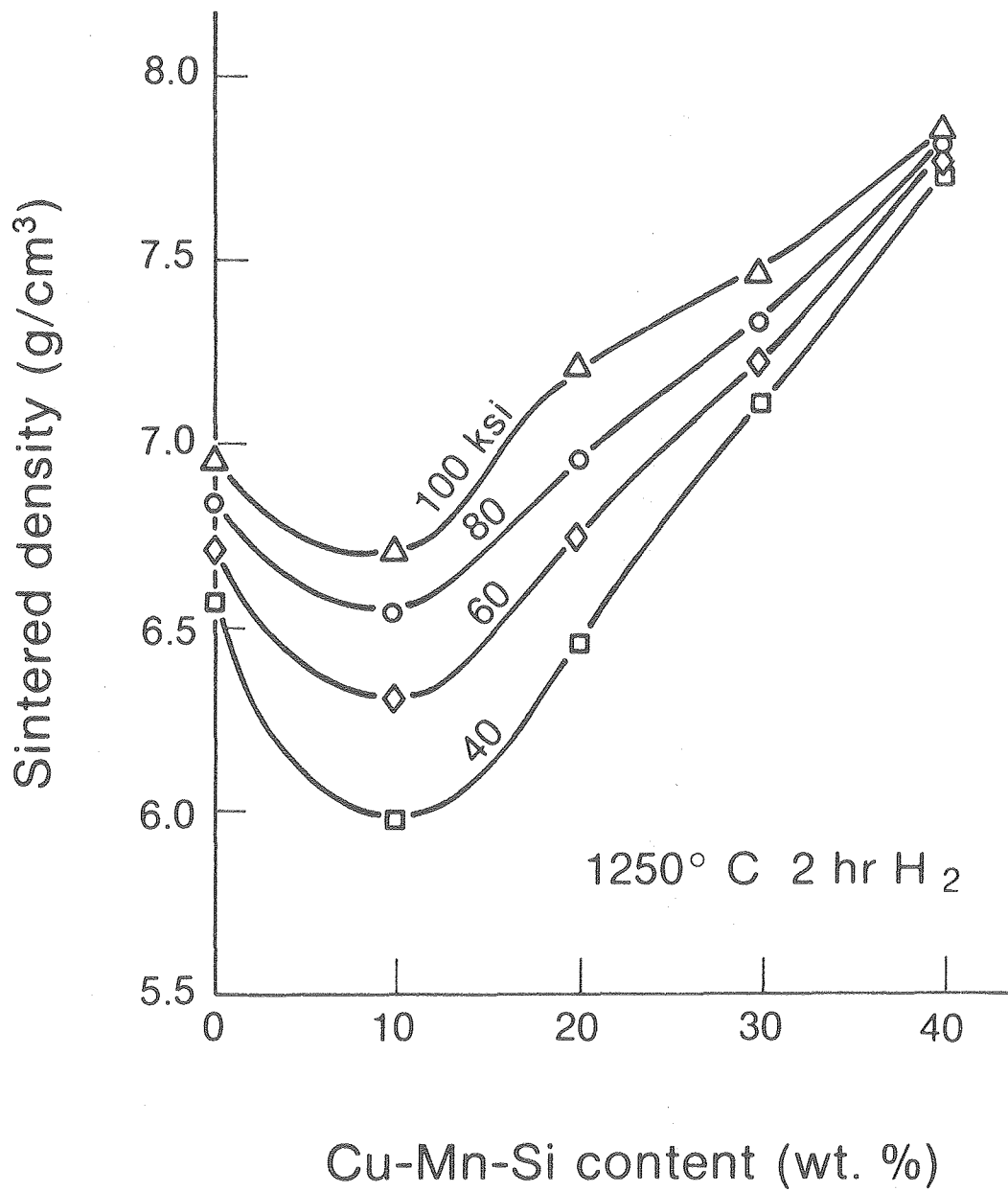
XBL 772 - 349

Fig. 7



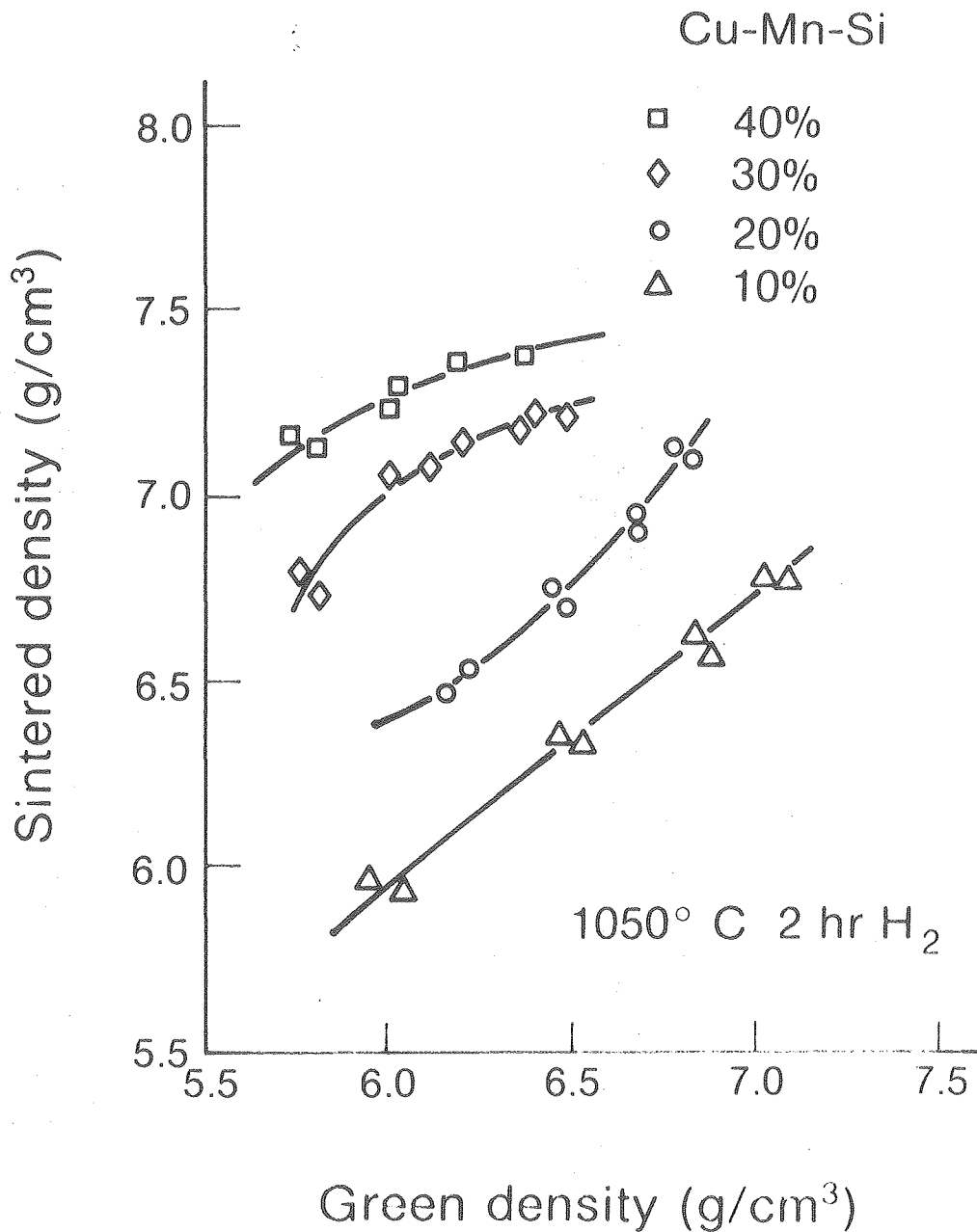
XBL 772-350

Fig. 8



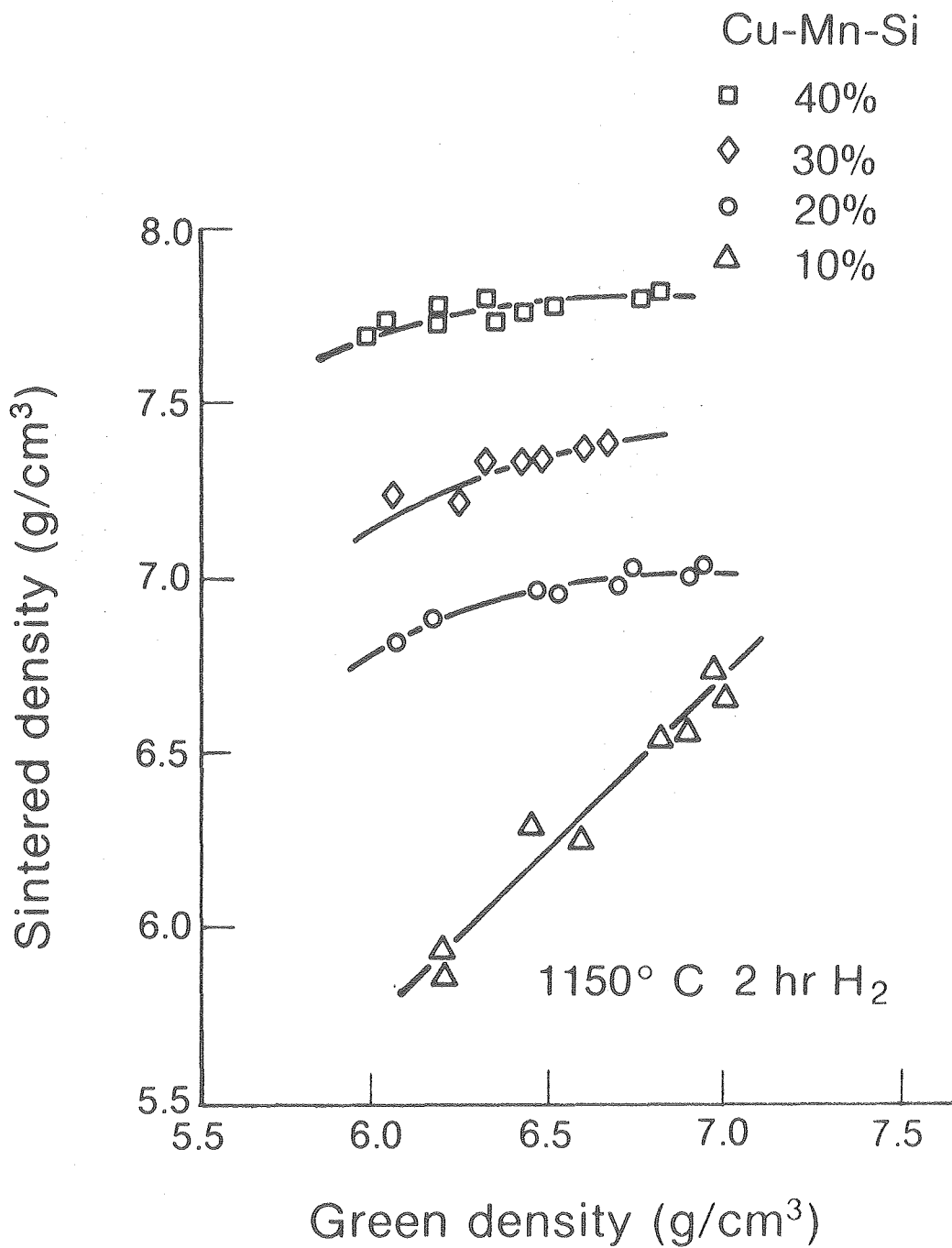
XBL 772-348

Fig. 9



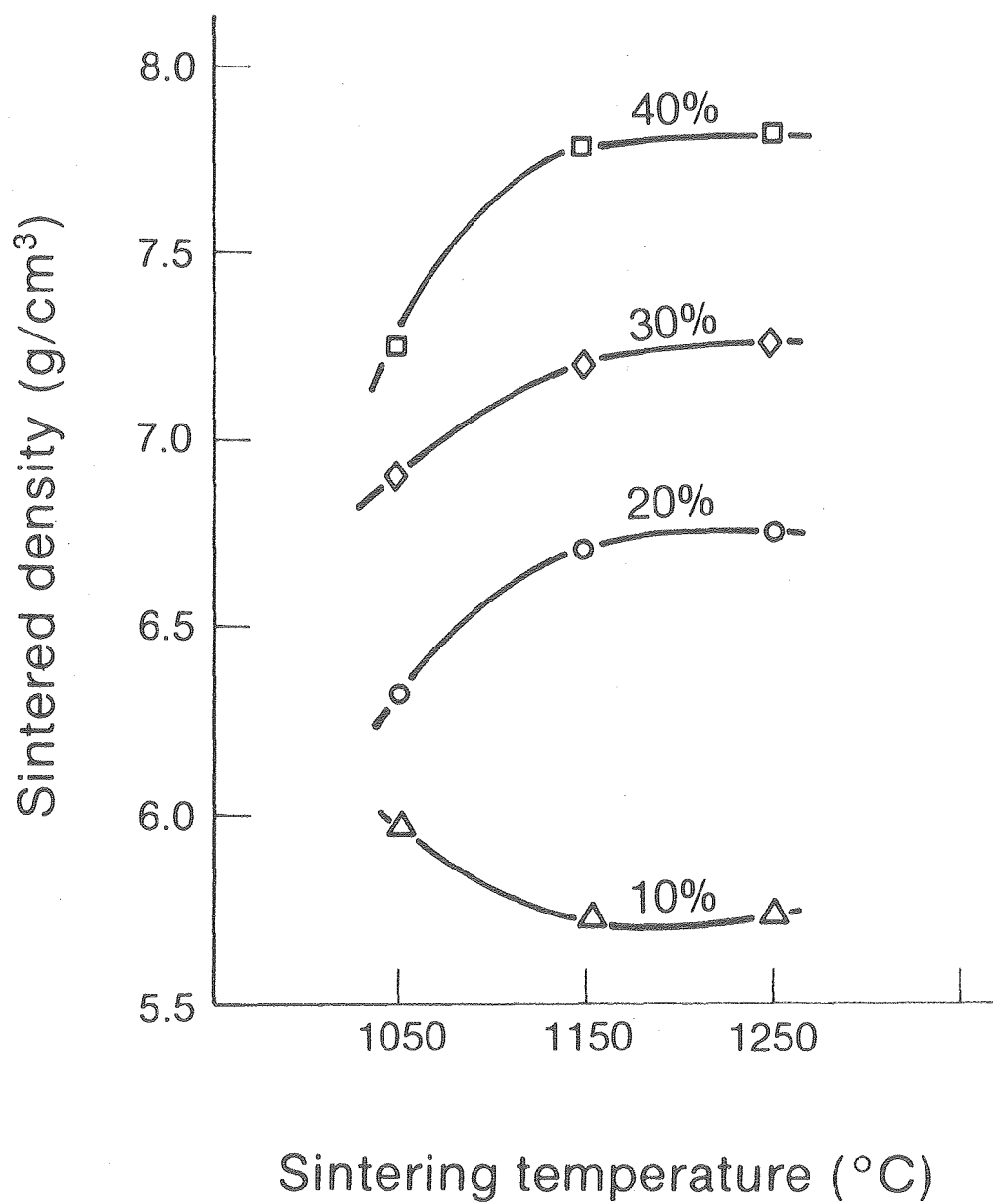
XBL 772-344

Fig. 10



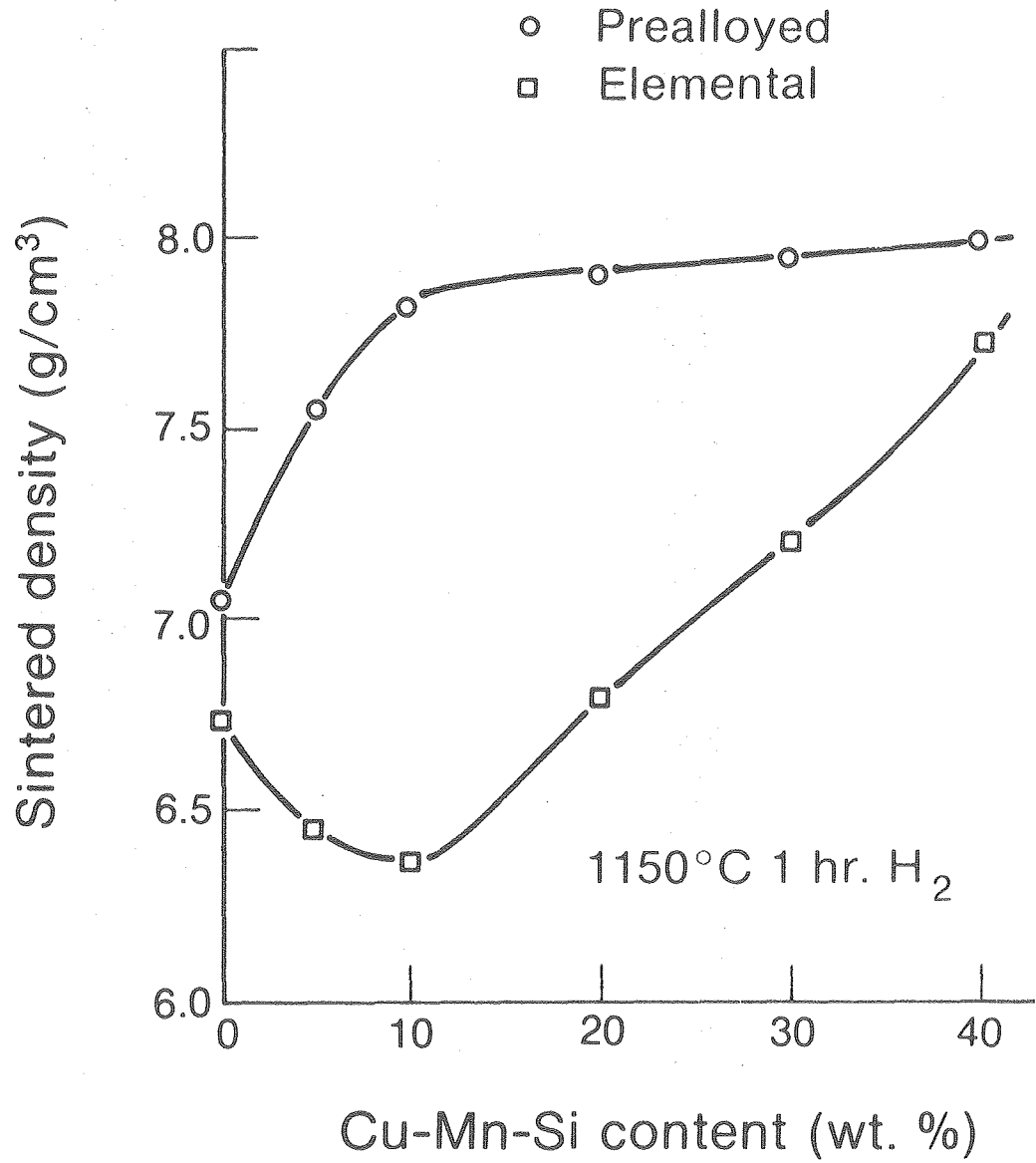
XBL 772-346

Fig. 11



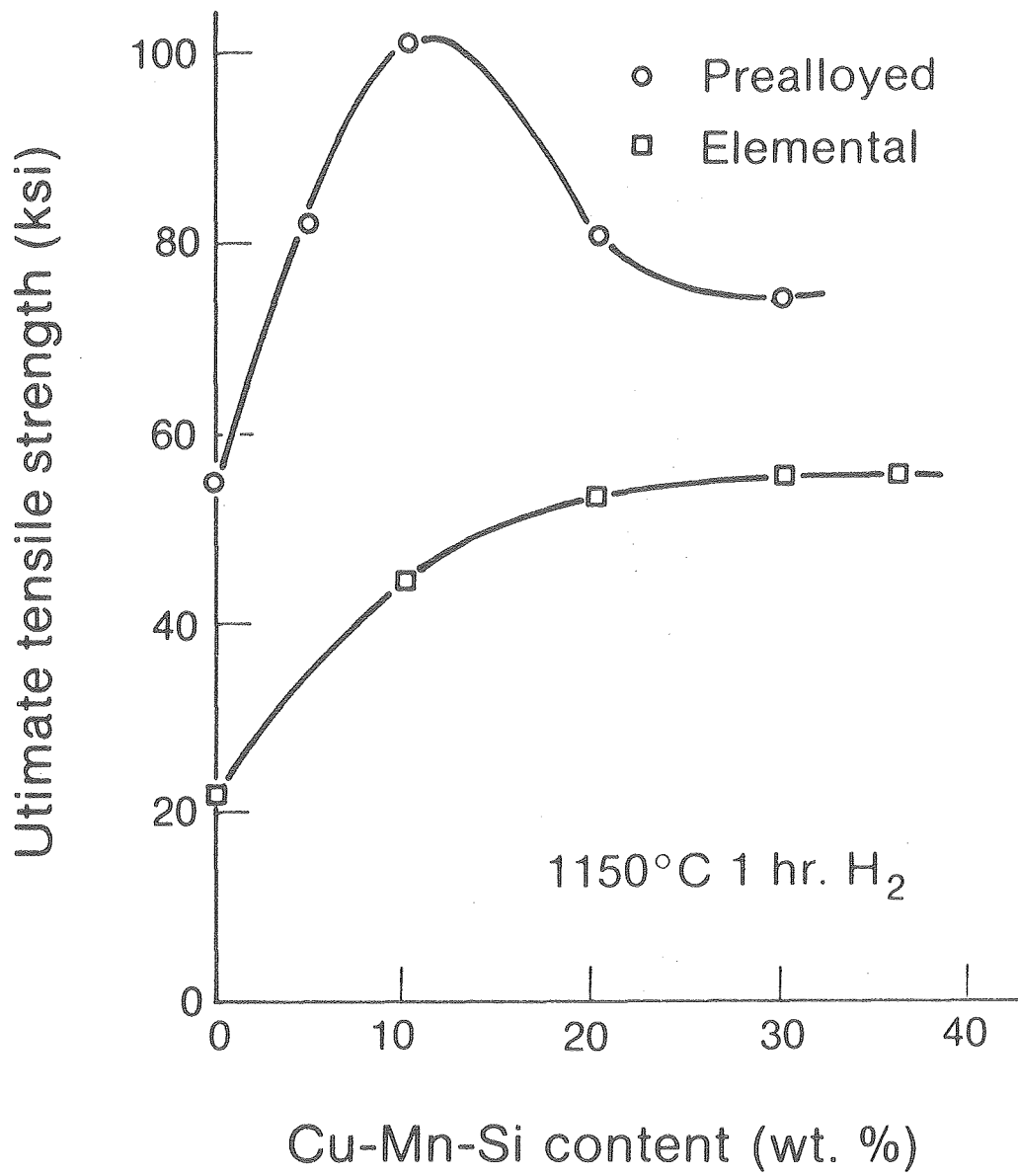
XBL 772-351

Fig. 13



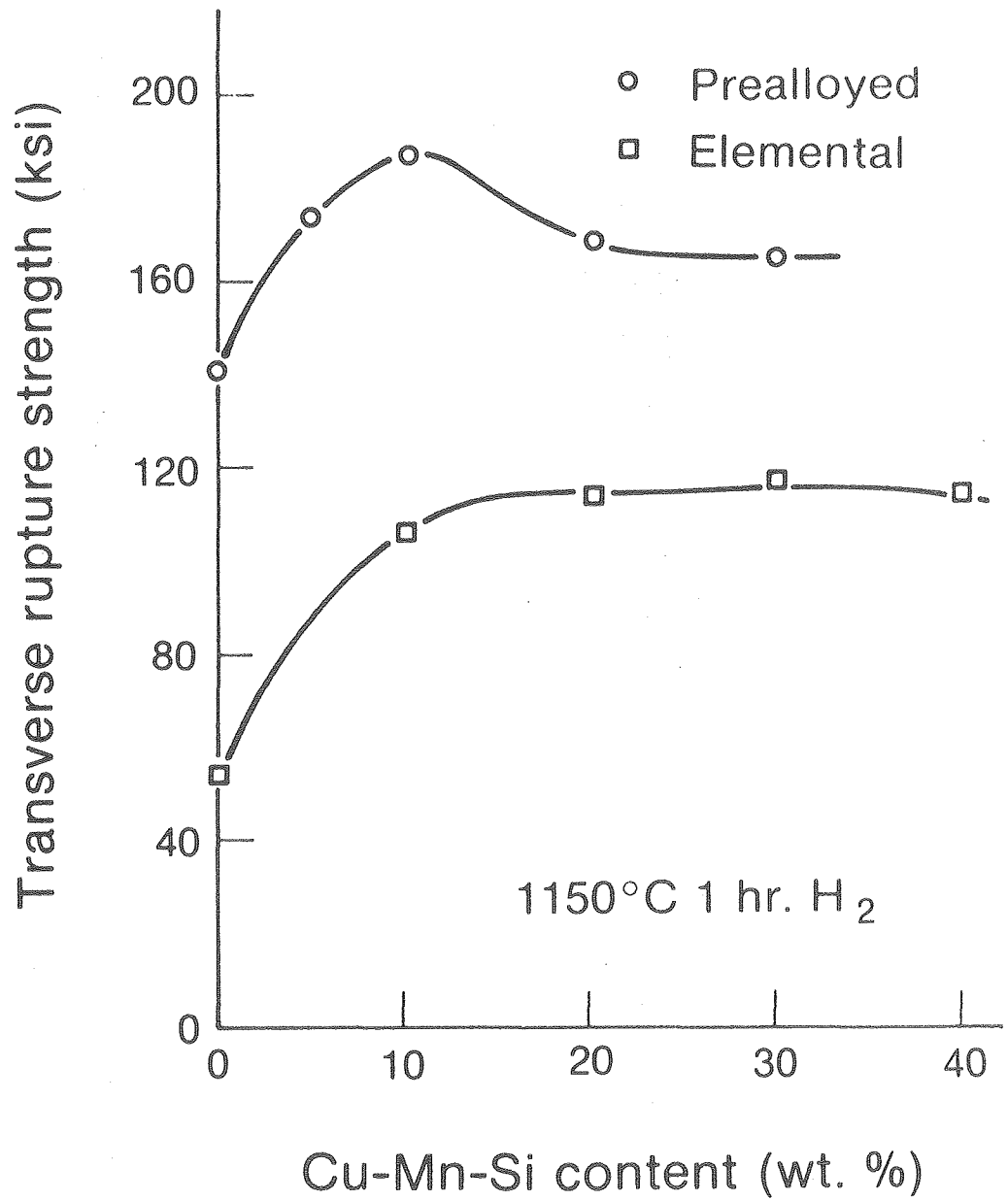
XBL 772-347

Fig. 14



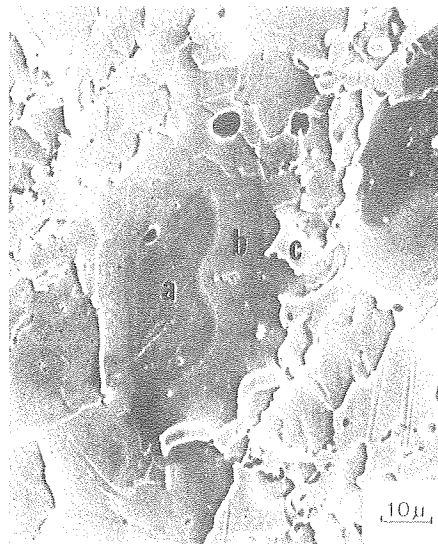
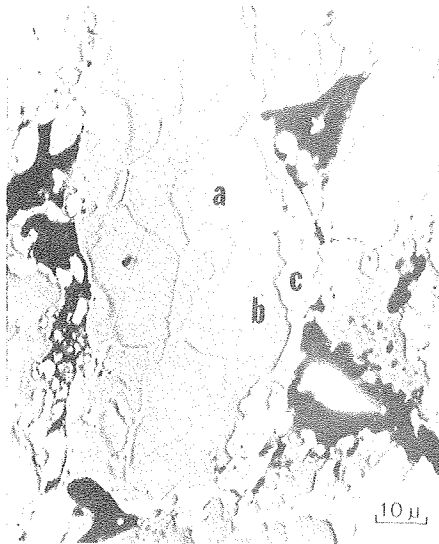
XBL 772-354

Fig. 15



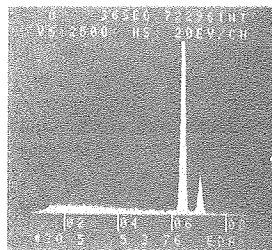
XBL 772-353

Fig. 16



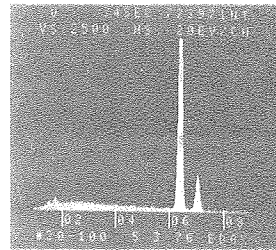
(a) Fe core

Fe 97.3
Cu 0.1
Mn 0.2
Si 2.4
VH 120



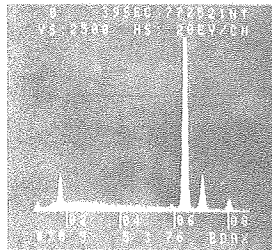
(a) Fe core

Fe 96.0
Cu 0.1
Mn 0.3
Si 3.6
VH 160



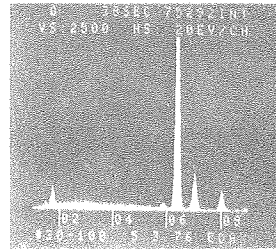
(b) Dif. zone

Fe 88.3
Cu 2.9
Mn 2.1
Si 6.1
VH 420



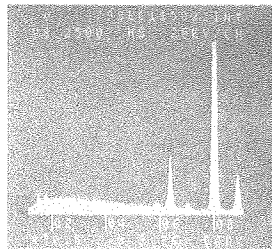
(b) Dif. zone

Fe 89.8
Cu 4.4
Mn 2.3
Si 4.5
VH 460



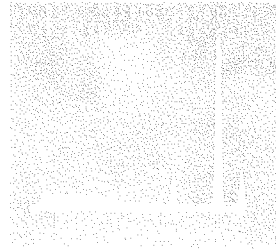
(c) Liquid

Fe 4.4
Cu 91.4
Mn 4.1
Si 0.1
VH 106



(c) Liquid

Fe 3.4
Cu 92.0
Mn 4.5
Si 0.1
VH 95



EMP - 30 % Cu-Mn-Si

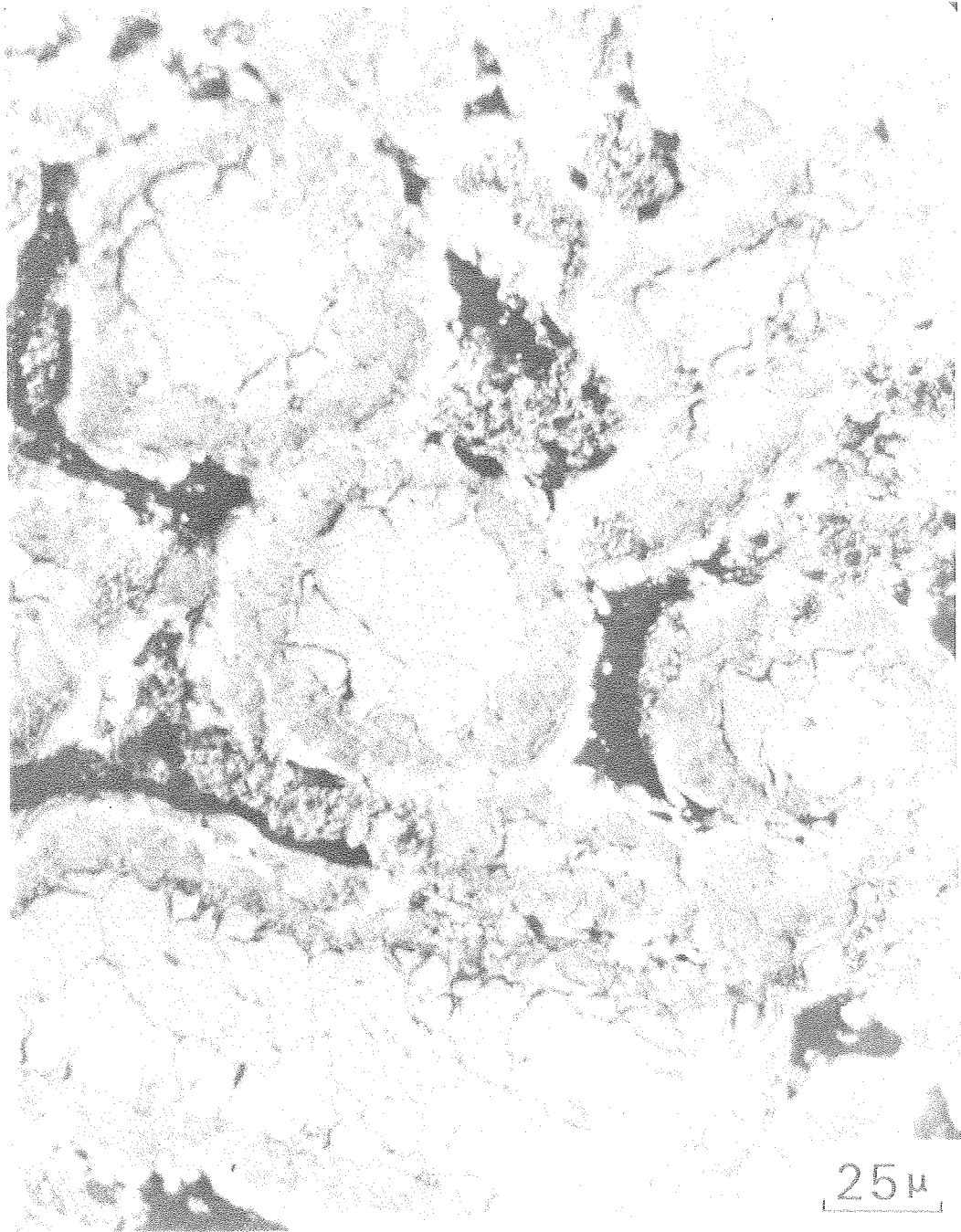
5 min, 1050°C H₂

EMP - 30 % Cu-Mn-Si

4 hr, 1050°C H₂

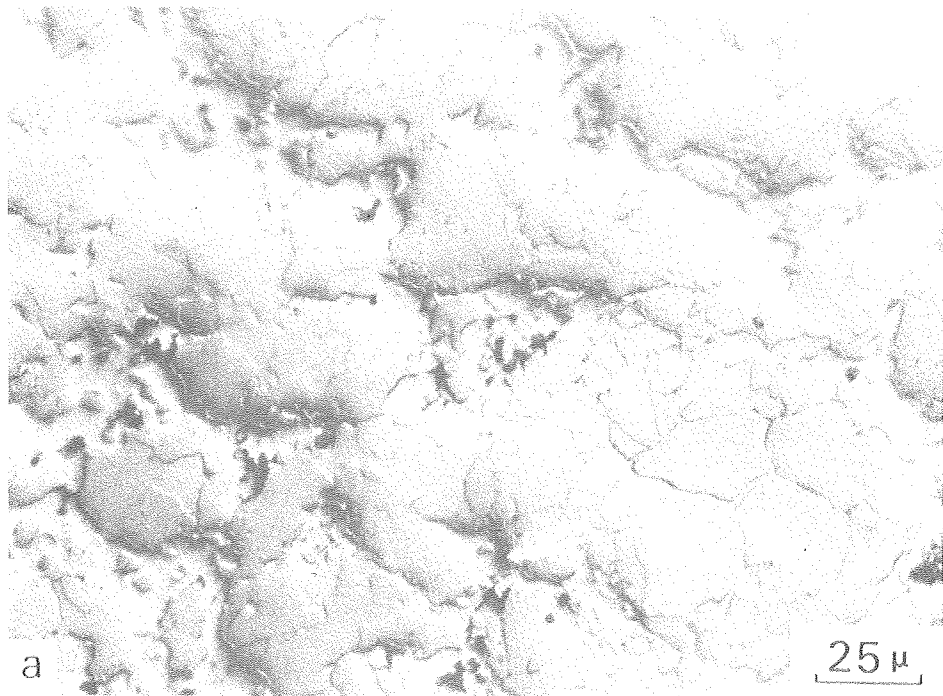
XBB 760-11752

Fig. 17



XBB 760-11750

Fig. 18



XBB 760-11749

Fig. 19

This report was done with support from the United States Energy Research and Development Administration. Any conclusions or opinions expressed in this report represent solely those of the author(s) and not necessarily those of The Regents of the University of California, the Lawrence Berkeley Laboratory or the United States Energy Research and Development Administration.